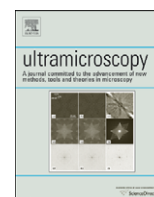




ELSEVIER

Contents lists available at ScienceDirect

## Ultramicroscopy

journal homepage: [www.elsevier.com/locate/ultramic](http://www.elsevier.com/locate/ultramic)

# Characterization of the tip-loading force-dependent tunneling behavior in alkanethiol metal–molecule–metal junctions by conducting atomic force microscopy

Hyunwook Song<sup>a</sup>, Hyoyoung Lee<sup>b</sup>, Takhee Lee<sup>a,\*</sup><sup>a</sup> Department of Materials Science and Engineering, Gwangju Institute of Science and Technology, Gwangju 500-712, Korea<sup>b</sup> National Creative Research Institute, Center for Smart Molecular Memory, IT Convergence Components Laboratory, Electronics and Telecommunications Research Institute, Daejeon 305-350, Korea

## ARTICLE INFO

## PACS:

85.65.+h

73.61.Ph

73.40.Gk

85.65.+h

## Keywords:

Self-assembled monolayers

Conducting atomic force microscopy

Molecular electronics

Tunneling

## ABSTRACT

We report on a tip-loading force-dependent tunneling behavior through alkanethiol self-assembled monolayers formed in metal–molecule–metal junctions, using conducting atomic force microscopy. The metal–molecule contacts were formed by placing a conductive tip in a stationary point contact on alkanethiol self-assembled monolayers under a controlled tip-loading force. Current–voltage characteristics in the alkanethiol junctions are simultaneously measured, while varying the loading forces. Tunneling current through the alkanethiol junctions increases and decay coefficient  $\beta_N$  decreases, respectively, with increasing tip-loading force, which results from enhanced intermolecular charge transfer in a tilted molecular configuration under the tip-loading effect.

© 2008 Elsevier B.V. All rights reserved.

## 1. Introduction

Electronic transport through self-assembled monolayers (SAMs) has recently become an active research area of scientific and technological interest [1–4]. For example, alkanethiol  $[\text{CH}_3(\text{CH}_2)_{n-1}\text{SH}]$  SAMs have been extensively studied, since they are self-assembled well on a Au(111) surface [5], which can provide a stable formation of metal–molecule contact. The transport properties through SAMs have, to date, been investigated utilizing various methods, such as mechanically controllable break junction [6], scanning tunneling microscopy (STM) [7], nanopore [8,9], conducting atomic force microscopy (CAFM) [10,11], electromigrated nanogap electrode [12,13], cross-wire tunnel junction [14], mercury-drop junction [15], nanorod [16], and others. Especially among them, the CAFM method has a key advantage for easy accessible junction formation, since no complicated fabrication procedure is required, and, unlike STM with vacuum tunnel gap, the CAFM provides a direct contact on a sample, so that a controlled tip-loading force can affect electronic properties in the molecules.

Here, we study a tip-loading force-dependent tunneling behavior through alkanethiol SAMs formed in metal–molecule–metal junctions using CAFM. A variable tip-loading force applies to alkanethiol

SAMs with a standard AFM feedback and current–voltage characteristics are simultaneously measured while varying the loading forces. In particular, we observe how a tip-loading force in CAFM has influence on tunneling characteristics of alkanethiol SAMs.

## 2. Experiment

### 2.1. Preparation of self-assembled monolayer

An  $\sim 5$  mM solution of alkanethiol was prepared in  $\sim 10$  mL anhydrous ethanol. All the chemicals were purchased from Sigma-Aldrich. The molecular deposition was done on Au surface (Au (250 nm)/Cr (3 nm)/glass) in solution for 1–2 days inside a nitrogen-filled glovebox, with an oxygen level of less than 20 ppm. Alkanethiols of various molecular lengths, octanethiol ( $\text{CH}_3(\text{CH}_2)_7\text{SH}$ , denoted as C8, for the number of alkyl units), dodecanethiol ( $\text{CH}_3(\text{CH}_2)_{11}\text{SH}$ , C12), and hexadecanethiol ( $\text{CH}_3(\text{CH}_2)_{15}\text{SH}$ , C16) were used to form the active molecular components. Before use, each sample was rinsed with a few mL of ethanol and gently blown dry in a stream of  $\text{N}_2$ .

### 2.2. Conducting atomic force microscopy measurement

Experiments were performed using a commercially available AFM system (PSIA, XE-100 model) with conductive AFM tips that

\* Corresponding author. Tel.: +82 62 970 2313; fax: +82 62 970 2304.  
E-mail address: [tlee@gist.ac.kr](mailto:tlee@gist.ac.kr) (T. Lee).

were made from a Au (20 nm)/Cr (20 nm) coating around conventional AFM tips. (Typical force constant of the cantilever from manufacturer specifications is 0.03 N/m.) Molecular junctions were prepared by placing a conductive AFM tip in the stationary point contact on alkanethiol SAMs under a controlled tip-loading force to define the contacts to the molecules [11]. An experimental schematic is shown in Fig. 1. Two terminal DC current–voltage ( $I(V)$ ) measurements were performed using a semiconductor parameter analyzer (HP4145B). Voltages were applied to the CAFM tip, while the Au substrate was grounded. All electrical measurements were carried out inside a covered AFM chamber in ambient through which nitrogen gas was being passed to minimize the formation of a contamination layer on SAM surface and to keep constant humidity (relative humidity 25–30%).

### 3. Results and discussion

A tip-loading force in the CAFM method influences the junction properties, because the CAFM tip is in direct contact with the molecules. For example, a tunneling current through the molecular junctions depends on a tip-loading force applied to a metal–molecules contact [11,17]. Fig. 2 shows force-dependent current–voltage characteristics of C12 SAMs when a tip-loading force is varied from 1 to 30 nN. All data were obtained with the same tip on the same sample position. The current through the molecular junction increased with increasing tip-loading force. A tip-loading force beyond 30 nN led to irreproducible results which were noisy and frequently electrically shorted. One would expect a mechanical breakdown of SAM structure under pressures over the load, and the consequent loss of their molecular properties. We therefore performed the CAFM experiments at forces of less than 30 nN.

It is instructive to check the current density of the molecular junction in demonstrating the force-dependent charge transport. At first glance, an increase in current with increasing loading

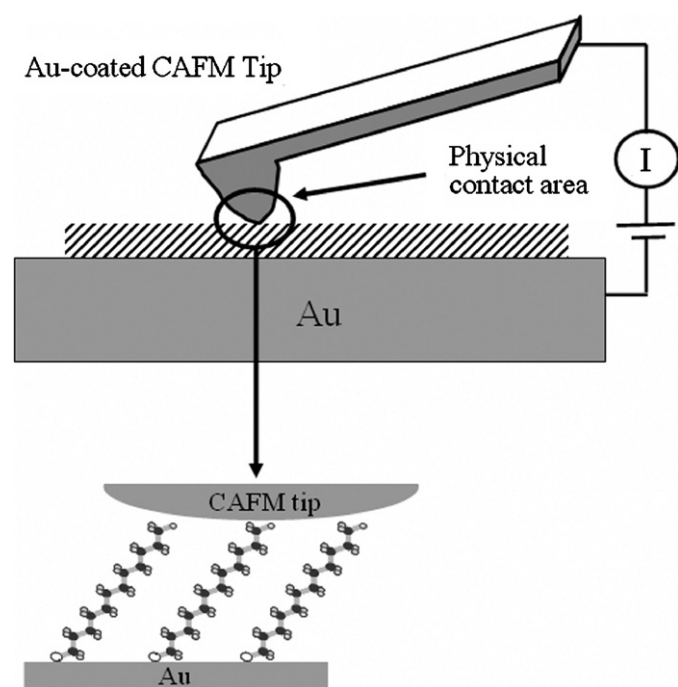


**Fig. 1.** A schematic of CAFM method used in this study. Chemical structures of dodecanethiol sandwiched between both Au electrodes, as an example of alkanethiols, are displayed.

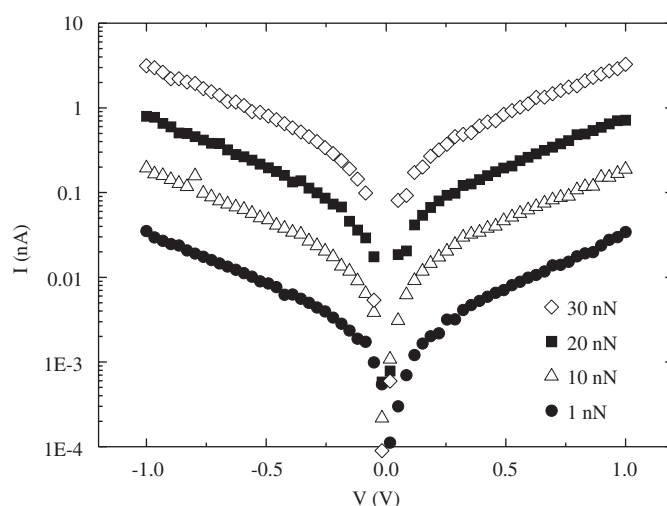


**Fig. 2.** Representative current–voltage characteristics of C12 SAMs for tip-loading forces varied from 1 to 30 nN.

force, as shown in Fig. 2, might be thought to result from the expansion of the tip–molecules contact area [11]. However, the current density should remain constant, if only the enlarged contact area contributes to an increase in current. The current density can be calculated by estimating a contact junction area for a given loading force. The Johnson–Kendall–Roberts (JKR) contact model [18] is typically used to evaluate the contact area [19,20]. The JKR contact model considers the interfacial adhesion force, which can be important at relatively small loads, and the model reflects the importance of interactions between the tip and the SAM [18]. According to the JKR contact model, the radius  $a$  of the junction area under the AFM tip contact is expressed by [18]

$$\begin{aligned} a^3 &= (R/K)P_n \\ &= (R/K)\{P + 3\Gamma\pi R + (6\Gamma\pi R P + (3\Gamma\pi R)^2)^{1/2}\} \end{aligned} \quad (1)$$

where  $R$  is the radius of the AFM tip end, as determined as about 35 nm by means of scanning electron microscope (SEM) images (a representative SEM image of Au-coated tip is shown in inset of Fig. 3) and  $K = (4/3)[(1-\nu_1^2)/E_1 + 1 - \nu_1^2/E_2]^{-1}$  where  $E_1$ ,  $\nu_1$ , and  $E_2$ ,  $\nu_2$  are Young's modulus and Poisson's ratio of the sample and the Au-coated tip, respectively. Appropriate  $E_1$ ,  $\nu_1$ ,  $E_2$ , and  $\nu_2$  are not available, but assuming  $E_1 \approx 10$  GPa [21,22],  $E_2 \approx 69$  GPa [23], and  $\nu_1 \approx \nu_2 \approx 0.33$  [19,24] compared with similar materials and structures,  $K$  can be calculated to be  $\sim 13$  GPa.  $P_n$  is the net force, which is the sum of the applied loading force  $P$  and terms due to the adhesion force.  $\Gamma = 2P_c/3\pi R$  is the adhesion energy per unit area related to the adhesion force  $P_c$  which can be obtained from a force–distance characterization. We obtained typical force–distance curves, from which adhesion forces ( $P_c$ ) of C8, C12, and C16 SAMs on Au substrate were determined to be 10.8, 12 and 13.5 nN, respectively.

As shown in Fig. 3, the current densities are not constant but, instead, gradually increase with increasing loading force. Here, the error bars were determined statistically from different measurements. Typically, we repeated the measurements 5–10 times on various sample positions to obtain one data point and the error bar. When the CAFM current–voltage measurements frequently produced an electric open or a short, we changed the CAFM tips or sample positions. The observation in Fig. 3 suggests that an increase in current is not simply due to an increase in the contact junction area, and thus a potential change in geometry of the molecules under the tip loads influences the electrical properties of the junctions [17,19].

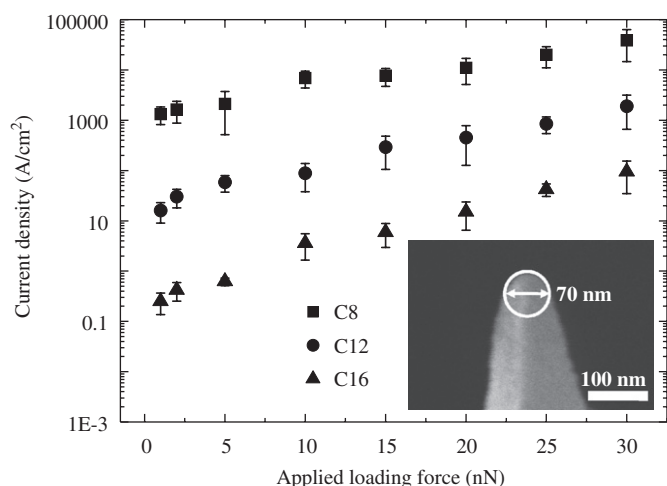


**Fig. 3.** A semilog plot of current densities at 1.0V for C8, C12, and C16 SAMs, as a function of applied tip-loading force. The inset shows a SEM image of Au-coated tip end.

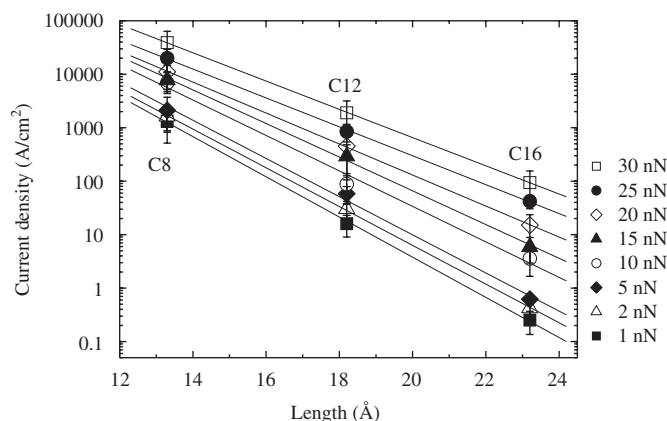


**Fig. 4.** A semilog plot of current densities at 1.0V versus the molecular length of C8, C12, and C16 SAMs for tip-loading forces varied from 1 to 30 nN. The linear lines through the data points are exponential fittings.

To understand the force-dependent tunneling transport through alkanethiol SAMs, length-dependent tunneling behavior was examined using different length alkanethiols while varying the tip-loading force. Electronic transport through alkanethiol SAMs is commonly described by a simple relation used for the tunneling mechanism as

$$J = J_0 \exp(-\beta_N d_m) \quad (2)$$

where  $J$  is current density flowing through the molecules,  $\beta_N$  is tunneling decay coefficient dependent on molecular structure, and  $d_m$  is molecular length, which is the width for the tunneling barrier.  $J_0$  indicates current density without the SAMs, which can be obtained by extrapolating to zero length from a logarithm plot of current density versus molecular length. Fig. 4 shows semilog plots of the current densities at 1.0V as a function of molecular lengths for a tip-loading force that was varied from 1 to 30 nN. Molecular lengths used in the analysis are 13.3, 18.2, and 23.2 Å for the C8, C12, and C16 alkanethiols, respectively. Each molecular length was determined by adding an Au-thiol bonding length to the length of molecule [25]. According to Eq. (2), the decay coefficient  $\beta_N$  can be determined from the slope of the exponential plots in Fig. 4. The results are displayed in Fig. 5. We found that  $\beta_N$  decreased with increasing loading force, while  $J_0$  was relatively uniform ( $\sim 1 \times 10^8$  A/cm<sup>2</sup>) irrespective of the tip-loading force. The magnitude of  $\beta_N$  is a critical factor in determining the efficiency of

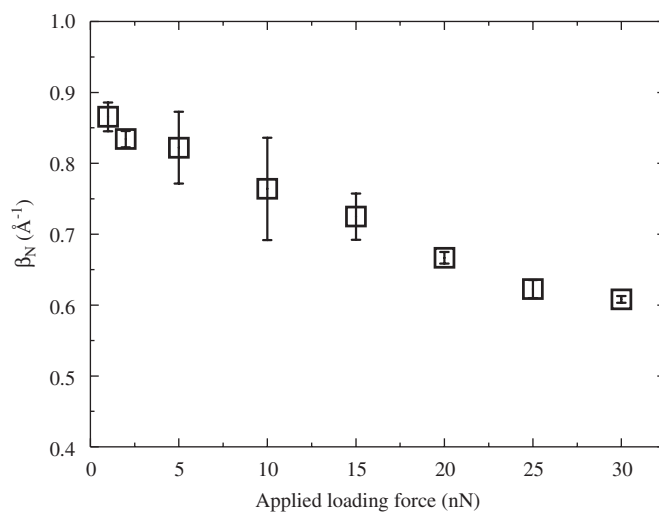


**Fig. 5.** A plot of the tunneling decay coefficient  $\beta_N$  from length-dependent experiment (from Fig. 4) versus the tip-loading force.

the tunneling process carrying charges through the molecules. The lower  $\beta_N$  value indicates a larger tunneling current through the barrier; in other words, more efficient tunneling. Therefore, an increase in tunneling current in Fig. 3 appears to be correlated with a decrease in  $\beta_N$  values with increasing loading force.

A molecular tilt angle with respect to a substrate normal would be expected to increase under a tip contact with certain loads, with the possible presence of other structural deformations (e.g., gauche configuration) [26]. Several authors have suggested the existence of an ordered tilted-chain phase of alkanethiol SAMs on Au(111) within the loading effect applied by the tip [27,28] and most of the deformation under a tip-loading force leads to additional tilting of the molecules [24,26]. It has also been reported that a tilted configuration of alkanethiol SAMs under tip-loading effect in CAFM method enhances intermolecular charge transfer [29]. This is because tunneling distance for intermolecular charge pathways decreases with the tilt of alkanethiol molecules [29]. Such an additional intermolecular tunneling process as the molecules tilt results in an increase in overall tunneling current and thus a decrease in decay coefficient  $\beta_N$ .

#### 4. Conclusion

The electronic transport in metal–alkanethiol–metal junctions was examined using CAFM. Tunneling current through alkanethiol SAMs increased and decay coefficient  $\beta_N$  obtained from different length alkanethiols decreased, respectively, with increasing tip-loading force in CAFM. Enhanced intermolecular charge transfer in the tilted molecular configuration under tip-loading effect is responsible for an increase in tunneling current and a decrease in decay coefficient  $\beta_N$ .

#### Acknowledgments

This work was supported by the National Research Laboratory (NRL) Program and the Basic Research Program of the Korea Science and Engineering Foundation, MIC & IITA (06-Infra-12, IT Research Infrastructure Program), and the Program for Integrated Molecular System at GIST. H.L. acknowledges the support of Creative Research Initiatives (Smart Molecular Memory) of MOST/KOSEF.

## References

- [1] M.A. Reed, T. Lee (Eds.), *Molecular Nanoelectronics*, American Scientific Publishers, Stevenson Ranch, CA, 2003.
- [2] G. Cuniberti, G. Fagas, K. Richter (Eds.), *Introducing Molecular Electronics*, Springer, Berlin (Heidelberg/New York), 2005.
- [3] E.A. Weiss, R.C. Chiechi, G.K. Kaufman, J.K. Kriebel, Z. Li, M. Duati, M.A. Rampi, G.M. Whitesides, *J. Am. Chem. Soc.* 129 (2007) 4336.
- [4] H.B. Akkerman, P.W.M. Blom, D.M. de Leeuw, B. de Boer, *Nature* 441 (2006) 69.
- [5] A. Ulman, *An Introduction to Ultrathin Organic Films from Langmuir-Blodgett to Self-Assembly*, Academic Press, Boston, 1991.
- [6] M.A. Reed, C. Zhou, C.J. Muller, T.P. Burgin, J.M. Tour, *Science* 278 (1997) 252.
- [7] Z.J. Donhauser, B.A. Mantooth, K.F. Kelly, L.A. Bumm, J.D. Monnell, J.J. Stapleton, D.W. Price Jr., A.M. Rawlett, D.L. Allara, J.M. Tour, P.S. Weiss, *Science* 297 (2001) 2303.
- [8] J. Chen, M.A. Reed, A.M. Rawlett, J.M. Tour, *Science* 286 (1999) 1550.
- [9] W. Wang, T. Lee, M.A. Reed, *Phys. Rev. B* 68 (2003) 035416.
- [10] X.D. Cui, A. Primak, X. Zarate, J. Tomfohr, O.F. Sankey, A.L. Moore, T.A. Moore, D. Gust, G. Harris, S.M. Lindsay, *Science* 294 (2001) 571.
- [11] D.J. Wold, C.D. Frisbie, *J. Am. Chem. Soc.* 123 (2001) 5549.
- [12] W. Liang, M.P. Shores, M. Bockrath, J.R. Long, H. Park, *Nature* 417 (2002) 725.
- [13] J. Park, A.N. Pasupathy, J.I. Goldsmith, C. Chang, Y. Yaish, J.R. Petta, M. Rinkoski, J.P. Sethna, H.D. Abruna, P.L. McEuen, D.C. Ralph, *Nature* 417 (2002) 722.
- [14] J.G. Kushmerick, D.B. Holt, S.K. Pollack, M.A. Ratner, J.C. Yang, T.L. Schull, J. Naciri, M.H. Moore, R. Shashidhar, *J. Am. Chem. Soc.* 124 (2002) 10654.
- [15] R. Holmlin, R. Haag, M.L. Chabinyc, R.F. Ismagilov, A.E. Cohen, A. Terfort, M.A. Rampi, G.M. Whitesides, *J. Am. Chem. Soc.* 123 (2001) 5075.
- [16] J.K.N. Mbindyo, T.E. Mallouk, J.B. Mattzela, I. Kratochvilova, B. Razavi, T.N. Jackson, T.S. Mayer, *J. Am. Chem. Soc.* 124 (2002) 4020.
- [17] K.A. Son, H.I. Kim, J.E. Houston, *Phys. Rev. Lett.* 86 (2001) 5357.
- [18] K.L. Johnson, K. Kendall, A.D. Roberts, *Proc. R. Soc. London A* 324 (1971) 301.
- [19] T. Lee, W. Wang, J.K. Klemic, J.J. Zhang, J. Su, M.A. Reed, *J. Phys. Chem. B* 108 (2004) 8742.
- [20] J. Zhao, K.J. Uosaki, *Phys. Chem. B* 108 (2004) 17129.
- [21] T.P. Weihs, Z. Nawaz, S.P. Jarvis, J.B. Pethica, *Appl. Phys. Lett.* 59 (1991) 3536.
- [22] R. Henda, M. Grunze, A.J. Pertsin, *Tribol. Lett.* 5 (1998) 191.
- [23] M.V. Salvadori, I.G. Brown, A.R. Vaz, L.L. Melo, M. Cattani, *Phys. Rev. B* 67 (2003) 153404.
- [24] X.D. Cui, X. Zarate, J. Tomfohr, O.F. Sankey, A. Primak, A.L. Moore, T.A. Moore, D. Gust, G. Harris, S.M. Lindsay, *Nanotechnology* 13 (2002) 5.
- [25] D.J. Wold, R. Haag, M.A. Rampi, C.D. Frisbie, *J. Phys. Chem. B* 106 (2002) 2813.
- [26] J.I. Siepmann, I.R. McDonald, *Phys. Rev. Lett.* 70 (1993) 453.
- [27] E. Barrena, C. Ocal, M.J. Salmeron, *Chem. Phys.* 113 (2000) 2413.
- [28] E. Barrena, C. Ocal, M.J. Salmeron, *Chem. Phys.* 114 (2001) 4210.
- [29] H. Song, H. Lee, T. Lee, *J. Am. Chem. Soc.* 129 (2007) 3806.